Electrochimica Acta, Vol. 36, No. 14, pp. 2135–2141, 1991
Printed in Great Britain.

0013-4686/91 $3.00 + 0.00

THE ANODIC DISSOLUTION OF 90% COPPER–10% NICKEL ALLOY IN HYDROCHLORIC ACID SOLUTIONS

F. K. CRUNDWELL
Dept of Chemical Engineering, University of the Witwatersrand, P.O. WITS, 2050 South Africa

(*Received* 5 *December* 1990; *in revised form* 19 *February* 1991)

Abstract—The anodic dissolution of the 90% copper–10% nickel alloy in hydrochloric acid solutions at the rotating disk was found to be controlled by both mass transfer and reaction in the apparent Tafel region. The kinetics of dissolution are similar to those of pure copper for the partial currents due to the dissolution of both the copper and nickel components from the alloy. A mechanism for the dissolution of the alloy is proposed. This mechanism describes the dissolution as being controlled by the dissolution of the copper from the alloy. In the limiting-current region a film of CuCl precipitates on the surface of the electrode. The reaction in the limiting-current region is controlled by mass transfer. A mechanism which describes the precipitation and dissolution of this film, and which describes the diffusion of the chloride to the surface of the electrode is proposed.

Key words: copper–nickel alloy, anodic dissolution, kinetics, rotating disk, hydrochloric acid.

INTRODUCTION

Copper–nickel alloys are widely used in marine environments because they exhibit resistance to corrosion in saline solutions. The dissolution of these alloys has been studied mainly with the view to elucidating the mechanism of the passivity in sulphate[1] and chloride[2–5] solutions.

The copper–nickel system has also attracted attention in fundamental studies of the dissolution of alloys. Bockris *et al.*[2] measured the partial currents due to the dissolution of Cu and Ni from the Cu–Ni alloy electrode as a function of the potential and the alloy composition in 1 M HCl solutions. They were able to evaluate the activities of the $CuCl_2^-$ and Ni^{2+} ions in solution and the activities of the Cu and Ni in the alloy, and from this they were able to evaluate the overpotentials, the rate constants, and the charge-transfer coefficients for each of the components of the alloy. Analysis of the variation of the transfer coefficient and the partial heats of activation with composition indicated the onset of phase separation above 55% Cu. This is confirmed by the thermodynamic study of Elford *et al.*[6] and the surface studies of Sakurai *et al.*[7] and Matsuyama *et al.*[8]. Bockris *et al.*[2], however, restricted their investigation to a discussion of the effect of alloy composition, and did not discuss the detailed kinetics of dissolution.

The kinetics of dissolution of the Cu 90%–Ni 10% alloy have been studied by Walton and Brook[3, 4]. They noted that the kinetics of dissolution of this alloy are similar to those for pure copper, but they did not propose a model for the mechanism of dissolution.

The anodic dissolution of copper in HCl solutions has been the subject of several investigations[9–17]. The polarization curves for the anodic dissolution of Cu in HCl solutions exhibit three distinct regions: the apparent-Tafel region, the limiting-current region, and a region anodic to the limiting-current region in which the current increases due to the formation of Cu^{2+}. In the apparent-Tafel region, the rate of dissolution is described by a mixed-kinetic model, in which the rate of reaction is controlled by both the reaction kinetics and the diffusion of $CuCl_2^-$ from the surface of the electrode. In this region, the Tafel slope is about 60 mV/decade, and the rate is proportional to $[Cl^-]^2$ and $\omega^{1/2}$, where ω is the rotation speed of the disk electrode. In the limiting-current region the rate of reaction is controlled by the diffusion of Cl^- to the surface of the electrode through a porous layer of CuCl that forms on the surface. In this region the rate is proportional to $[Cl^-]$ and $\omega^{1/2}$.

The anodic dissolution of nickel in HCl solutions has been studied in detail by Bengali and Nobe[18]. They reported a Tafel slope of about 75 mV/decade, and that at low chloride concentrations the rate was proportional to $[Cl^-]^{1/2}$, while at high chloride concentrations the rate was proportional to $[Cl^-]$. However, Bockris *et al.*[2] reported a Tafel slope of 105 mV/decade for the dissolution of pure nickel.

In this paper we report the results of the steady-state investigation of the anodic dissolution of Cu 90%–Ni 10%, and provide a model for the mechanism of dissolution in both the apparent-Tafel region, and in the limiting current region. The model for the dissolution of copper from the alloy in the limiting-current region is discussed. This model has important consequences for the interpretation of the *ac*-impedance results. These *ac*-impedance results will be presented in a subsequent paper.

EXPERIMENTAL

A rotating ring-disk electrode assembly was used for all the potential-sweep and steady-state measurements. The electrode consisted of a 90% copper–10% nickel disk with a diameter of 0.35 cm and a platinum

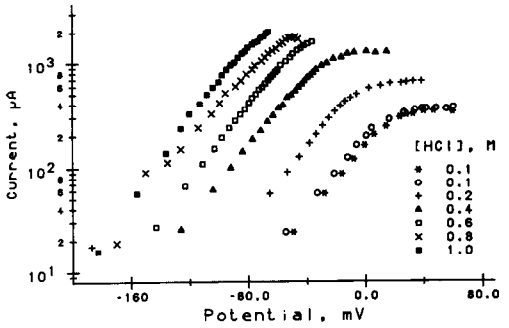

Fig. 1. The effect of the concentration of HCl on the rate of dissolution of copper from the alloy. Sweep rate 0.18 mV s^{-1}, rotation speed 500 rpm.

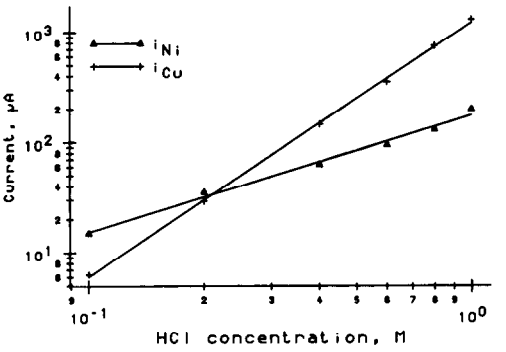

Fig. 3. The effect of the concentration of HCl on the partial currents due to copper and nickel dissolution in the apparent-Tafel region. i_{Cu} at −75 mV, and i_{Ni} at −80 mV.

ring. The electrode was constructed so that a gap between the ring and the disk was filled with Araldite epoxy, and these two electrodes were inserted in a teflon holder. The counter electrodes were made of platinum. A saturated calomel electrode was used as the reference and all potentials are referred to this electrode. The collection efficiency of the ring was determined to be 0.37. The electrode was polished with 1200 grit waterpaper and less than 5 μm alumina paste prior to each experiment.

Analytical grade hydrochloric acid and deionized water were used. All experiments were at 25°C.

The potentiostats and potential-sweep generator were manufactured at MINTEK, and the currents and potentials were recorded on an HP 7090A measurement system. The ring potential was set to +610 mV *vs sce* to detect cuprous ions by oxidizing them to cupric ions, and set to −100 mV *vs sce* to detect cupric ions in the limiting-current region by reducing them to cuprous ions. The sweep rate at the disk was maintained at 0.18 mV s^{-1}. Steady-state measurements were made once the current had stabilized. The electrode typically took 5–25 minutes to achieve steady-state.

RESULTS

Results for the potential-sweep investigation of the anodic dissolution of a Cu 90%–Ni 10% alloy from a rotating-disk electrode are shown in Figs 1 and 2. Figure 1 shows the partial current due to the dissolution of the copper component from the alloy, and Fig. 2 shows the partial current due to the dissolution of the nickel component from the alloy. The results shown in Fig. 1 illustrate that the partial current due to copper dissolution displays an apparent-Tafel region with a slope of between 55 and 60 mV/decade and a limiting-current region at higher anodic potentials. The results for the partial current due to nickel dissolution are more scattered, but are roughly linear with a slope between 75 and 105 mV/decade. Both these figures indicate that the partial currents for each of the components are strongly dependent on the chloride concentration. Figure 3 illustrates the effect of the chloride concentration on the partial currents for the dissolution of copper and nickel, taken from Figs 1 and 2. The partial copper current is proportional to $[Cl^-]^{2.3}$, while the partial nickel current is proportional to $[Cl^-]^{1.05}$.

The partial current due to the dissolution of copper from the alloy is dependent on the stirring conditions. This is illustrated in Fig. 4. This current is proportional to $\omega^{0.41}$. The anodic dissolution of pure copper is known to exhibit a strong dependence on the stirring conditions. The effect of the partial nickel current on the rotation speed of the disk electrode is shown in Fig. 5. This figure indicates that the partial current due to nickel dissolution is independent of the rotation speed under the conditions of the potential-sweep investigation. These results have a Tafel slope of 75 mV/decade, which is the same as that given by Bengali and Nobe[18] for the dissolution of pure nickel.

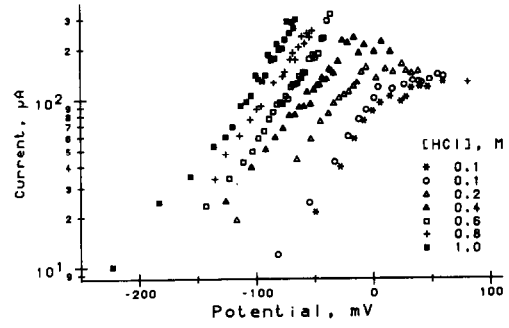

Fig. 2. The effect of the concentration of HCl on the rate of dissolution of nickel from the alloy. Sweep rate 0.18 mV s^{-1}, rotation speed 500 rpm.

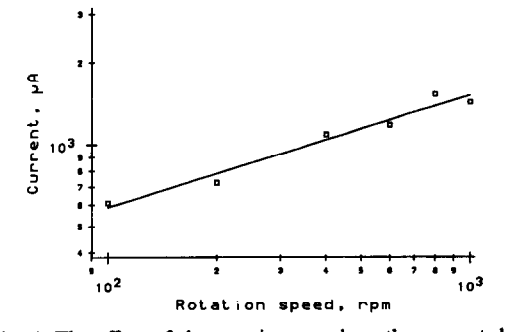

Fig. 4. The effect of the rotation speed on the current due to copper dissolution in the apparent-Tafel region. 1.0 M HCl, −90 mV.

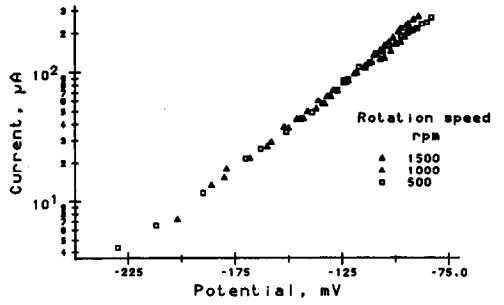

Fig. 5. The effect of the rotation speed on the current due to nickel dissolution in the apparent-Tafel region. 1.0 M HCl, sweep rate 0.18 mV s^{-1}.

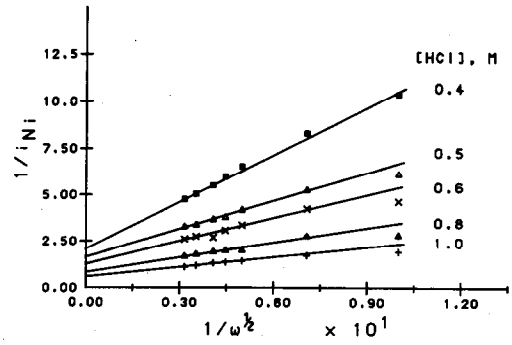

Fig. 7. The effect of the rotation speed on the current due to nickel dissolution in the apparent-Tafel region (− 60 mV) at steady state.

The results for the potential-sweep investigation indicate that the partial current due to copper dissolution is controlled by both reaction kinetics and diffusion in the apparent-Tafel region, while the partial current due to nickel dissolution is controlled by reaction kinetics in the same potential region. The kinetic parameters obtained for each component are similar to those for the dissolution of the pure metals, suggesting that the dissolution of each component is independent of the other component.

The dissolution of the alloy electrode was also investigated using steady-state techniques.

Mixed-control kinetics at a rotating-disk electrode such as those observed for the partial current due to the dissolution of copper from the alloy are normally analysed by plotting the results according to equation (1),

$$\frac{1}{i} = \Upsilon\frac{1}{\omega^{1/2}} + \frac{1}{i^{\infty}}, \qquad (1)$$

where i is the current. The slope of the plot of $1/i$ against $1/\omega^{1/2}$, Υ, is dependent on both mass transfer and kinetic factors, while the inverse of the intercept, i^{∞}, is the current as $\omega \to \infty$, that is, when mass transfer effects are negligible. It is possible in this way to eliminate the effects of mass transfer and to obtain the parameters affecting the reaction kinetics.

The effect of the rotation speed on the current at constant potential is shown in Figs 6 and 7 for the partial currents due to copper and nickel dissolution, respectively. These figures indicate that the dissolution of each component from the alloy is described by equation (1). These figures emphasize the strong dependence this reaction has on the rotation speed and on the chloride concentration. The results of Fig. 7 are slightly curved; this may be the result of the simultaneous dissolution of copper and nickel interfering slightly with each other, or another simultaneous process that may be occurring.

The dependence of the inverse of the intercept of equation (1), i^{∞}, and the slope, Υ, on the HCl concentration for the partial currents due to the dissolution of copper and nickel from the alloy are shown in Figs 8 and 9, respectively. Both the copper and the nickel partial currents show similar kinetic results, *ie*, i^{∞}_{Cu} is proportional to $[Cl^-]^{1.55}$, and i^{∞}_{Ni} is proportional to $[Cl^-]^{1.4}$, while Υ_{Cu} is proportional to $[Cl^-]^{1.91}$ and Υ_{Ni} is proportional to $[Cl^-]^{-1.91}$.

The effect of the rotation speed on the current at constant HCl concentration was also investigated. These results were plotted according to equation (1), and the dependence of the slope, Υ, and the inverse of the intercept, i^{∞}, on the potential is shown in Figs 10 and 11 for the partial currents due to copper and nickel dissolution, respectively. Both the copper and nickel partial currents show similar kinetic results, *ie*, i^{∞}_{Cu} has dependence of 118 mV/decade and i^{∞}_{Ni} has a dependence of 114 mV/decade, while Υ_{Cu} has a dependence of −65 mV/decade and Υ_{Ni} has a dependence of −60 mV/decade.

These results indicate that the dissolution of copper and nickel from the alloy are not independent of each other, since at steady state the dissolution of these two components from the alloy follow the same

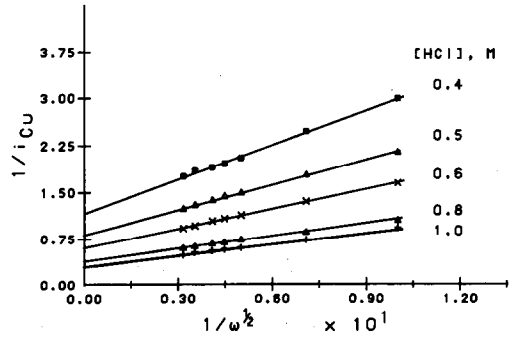

Fig. 6. The effect of the rotation speed on the current due to copper dissolution in the apparent-Tafel region (− 60 mV) at steady state.

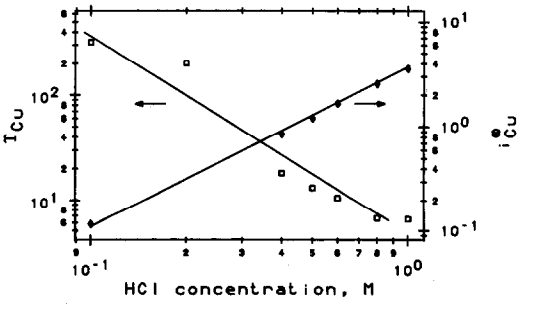

Fig. 8. The effect of the concentration of HCl on the slope, Υ, and the inverse of the intercept, i^{∞}, of the plot for the partial copper current.

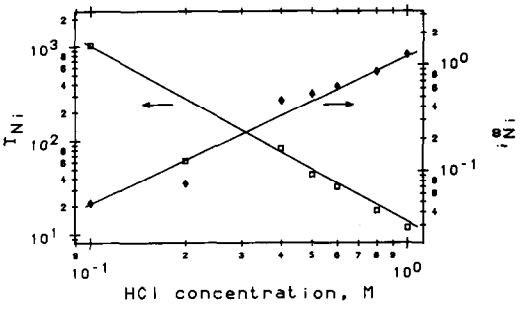

Fig. 9. The effect of the concentration of HCl on the slope, Υ, and the inverse of the intercept, i^{∞}, of the plot for the partial nickel current.

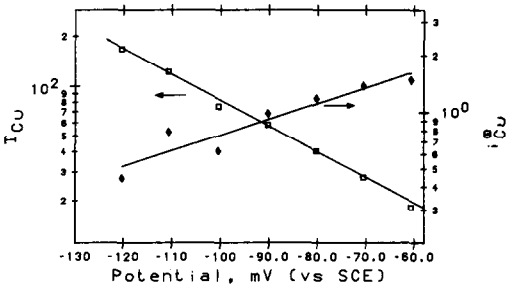

Fig. 10. The effect of the potential on the slope, Υ, and the inverse of the intercept, i^{∞}, of the plot for the partial copper current.

kinetics. This would seem to contradict the findings of potential-sweep investigation, *ie* that the dissolution of each component is independent of each other.

The results for the steady-state investigation of the dissolution of the alloy in the limiting-current region are shown in Figs 12 and 13. Figure 12 indicates that the copper partial current is proportional to $[Cl^-]^{1.06}$ while the nickel partial current is proportional to $[Cl^-]^{0.5}$. Figure 13 indicates that the copper partial current is proportional to $\omega^{0.47}$ while the nickel partial current is proportional to $\omega^{0.2}$.

A substantial layer of CuCl was detected in the limiting-current region in the following way. The ring potential was set at 610 mV to record the rate of formation of the cuprous species. When the disk current was switched off, the dissolution of the film continued, and was detected at the ring. The area under the ring current–time curve is a measure of the relative film thickness.

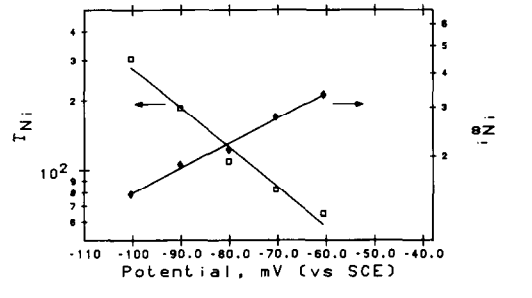

Fig. 11. The effect of the potential on the slope, Υ, and the inverse of the intercept, i^{∞}, of the plot for the partial nickel current.

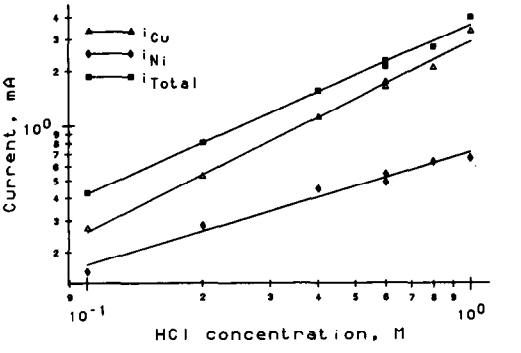

Fig. 12. The effect of the concentration of HCl on the total current and on partial currents due to copper and nickel dissolution in the limiting-current region. 40 mV, 500 rpm.

These results suggest that in the limiting-current region the dissolution of each of the components obeys the kinetics for the pure component at low chloride concentrations. The current due to the dissolution of the copper from the alloy follows kinetics similar to that of copper in the limiting-current region, *ie* first-order in $[Cl^-]$ and proportional to $\omega^{1/2}$, while the dissolution of the nickel component follows kinetics similar to that of pure nickel at low concentrations of Cl^-, *ie* half-order in $[Cl^-]$ and independent of the agitation.

DISCUSSION

The selective dissolution of one or more of the elements from an alloy is a well-known phenomenon, and is a process that is considered an important factor in stress-corrosion cracking. In an alloy where the components dissolve at rates that are not stoichiometric ratios of each other, a new phase may form on the surface of the alloy. Bockris *et al.*[2] postulated the formation of new phases on the surface of Cu–Ni alloys with compositions 65% Cu and above.

The potential-sweep experiments performed in this study took about 25 min for a complete scan, while the steady-state measurements often took about 10 min for the current to stabilize. Therefore, the potential-sweep experiments were not at steady-state, probably because a new phase on the surface of the alloy (due to the dissolution of a stoichiometric excess

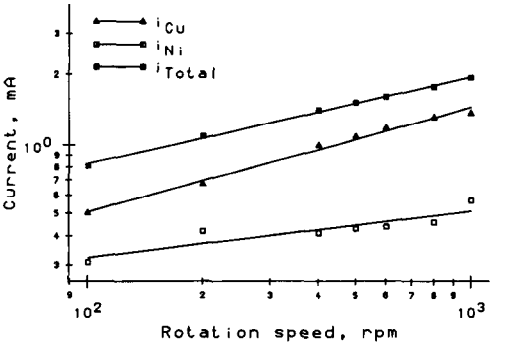

Fig. 13. The effect of the rotation speed on the total current and on the partial currents due to copper and nickel dissolution in the limiting-current region. 0.5 M HCl, 40 mV.

of the less noble component, Ni) was not fully developed.

The different kinetics reported here for the potential-sweep and steady-state investigations can be understood in these terms. The new phase on the surface of the alloy is not developed under the conditions of the potential-sweep experiments, so each component dissolves independently of each other, giving rise to kinetics similar to those of the pure components. This phase on the surface of the alloy is fully developed under the conditions of the steady-state experiments, so the ratio of the partial currents for the dissolution of each component is close to the molar ratio of the alloy composition and the kinetics of dissolution are the same for each component and are similar to that for the dissolution of pure copper. This suggests that the phase on the surface of the alloy may be rich in copper and that the kinetics of dissolution of the alloy are limited by the dissolution of this copper-rich phase. In the limiting-current region the kinetics of dissolution are dissimilar for each component, suggesting that each component dissolves independently. This may be because there is no formation of the copper-rich phase on the surface of the electrode.

The analysis of the kinetics of dissolution of the alloy at steady state for the apparent-Tafel region and for the limiting-current region are discussed in further detail below.

Apparent-Tafel region

The dissolution of the copper and nickel components from the alloy have the same kinetic parameters, which are also the same as those for the dissolution of pure copper. For this reason the kinetic expression developed here is the same as that developed for the dissolution of pure copper.

The mechanism of the anodic dissolution of Cu from the alloy in Cl^- solutions in the apparent-Tafel region can be expressed as a two-step reaction:

$$Cu + Cl^- \underset{k_{-1}}{\overset{k_1}{\rightleftharpoons}} CuCl_{ads} + e^- \qquad (2)$$

$$CuCl_{ads} + Cl^- \underset{k_{-2}}{\overset{k_2}{\rightleftharpoons}} CuCl_2^- . \qquad (3)$$

$CuCl_{ads}$ represents an intermediate cuprous chloride species which is adsorbed onto the copper electrode surface. The concentration gradient of $CuCl_2^-$, C_1, is determined by convective diffusion:

$$\frac{\partial C_1}{\partial t} = D_1 \frac{\partial^2 C_1}{\partial x^2} - v_x \frac{\partial C_1}{\partial x}, \quad x > 0. \qquad (4)$$

This differential equation is subject to the following boundary conditions:

$$x = 0,\ N_1(0) = k_2 \theta C_2(0) - k_{-2} C_1(0) \qquad (5)$$

$$x = \infty,\ C_1(\infty) = 0, \qquad (6)$$

where $N_1(0)$ is the flux of $CuCl_2^-$ at the surface, θ is the surface coverage of the $CuCl_{ads}$ adsorbed intermediate, and $C_2(0)$ is the concentration of Cl^- at the surface.

The rate of the electrochemical reaction (2) is given by

$$\frac{i}{F} = k_1 C_2(0)(1-\theta) - k_{-1}\theta. \qquad (7)$$

The electrochemical rate constants k_1 and k_{-1} are dependent on the potential.

The rate of formation of $CuCl_{ads}$ is governed by the mass balance equation

$$\frac{d\theta}{dt} = \frac{i}{F} - k_2 C_2(0)\theta + k_{-2} C_1(0). \qquad (8)$$

Equation (8) yields the expression for the steady-state surface coverage by $CuCl_{ads}$, θ.

$$\theta = \frac{i/F + k_{-2} C_1(0)}{k_2 C_b}. \qquad (9)$$

If it is assumed that θ is sufficiently small so that $(1-\theta) \approx 1$, and that the chloride concentration at the surface is the same as the bulk concentration, so that $C_2(0) = C_b$, then equation (7) becomes

$$\frac{i}{F} = k_1 C_b - k_{-1}\theta. \qquad (10)$$

The $CuCl_2^-$ concentration gradient is given by equation (4) and the boundary conditions, equations (5) and (6). Solving equations (4) and (9) for $C_1(0)$ and θ and substituting these expressions into equation (10) with $k_1 = k_1' \exp\{\alpha FE/RT\}$ and $k_{-1} = k_{-1}' \exp\{-(1-\alpha)FE/RT\}$, and $\delta = 1.805 D_1'^{1/3} \nu^{1/6} \omega^{-1/2}$, gives

$$\frac{F}{i} = \frac{1}{k_1' C_b \exp\{\alpha FE/RT\}} + \frac{k_{-1}'}{k_1' k_2 C_b^2 \exp\{FE/RT\}} + \frac{k_{-1}' k_{-2} \tau \omega^{-1/2}}{k_1' k_2 C_b^2 \exp\{FE/RT\}}, \qquad (11)$$

where $\tau = 1.805 D_1'^{-2/3} \nu^{1/6}$, and ν is the viscosity.

If this equation is plotted in the form of equation (1) it indicates that i^∞ should be proportional to $[Cl^-]^x$ where x is between 1 and 2, and should have a potential dependence between 60 and 120 mV/decade. In addition it predicts that Υ should be proportional to $[Cl^-]^{-2}$ and have a potential dependence of -60 mV/decade. Figures 6 to 11 indicate that both the copper and nickel partial currents obey equation (11).

Limiting-current region

At higher current densities a porous CuCl layer forms on the copper surface. The formation of this layer is associated with the limiting-current plateau. It is generally agreed[9, 10, 16, 17] that the reaction is controlled by the diffusion of Cl^- in this potential region, *ie* there is a change of mechanism between the apparent-Tafel region and the limiting-current region. This change of mechanism suggests that film formation is not due to a mechanism where the rate of diffusion of $CuCl_2^-$ from the electrode cannot match the rate of $CuCl_2^-$ production, (with the result that saturation occurs, and crystalline CuCl precipitates on the electrode surface), but rather that film formation is due to a mechanism where the rate of diffusion of Cl^- cannot match the rate of production of $CuCl_2^-$. The product of the reaction under these conditions is aqueous CuCl, and since the solubility

of CuCl is low, crystalline CuCl precipitates at the surface of the electrode, and this initiates the growth of a porous film. This process can be represented by reaction (2) together with the reaction

$$CuCl_{ads} \xrightarrow{k_3} CuCl_{(film)}. \quad (12)$$

The adsorbed species $CuCl_{ads}$ may not be the direct precursor to the precipitation of crystalline CuCl; it may be that this is aqueous CuCl. However, the analysis following is the same whether we refer to this species as aqueous CuCl (provided the product of reaction (2) is aqueous CuCl, which precipitates in the vicinity of the electrode–salt interface) or as adsorbed $CuCl_{ads}$. This porous film dissolves chemically at the solution-film boundary:

$$CuCl + Cl^- \underset{k_{-4}}{\overset{k_4}{\rightleftharpoons}} CuCl_2^-. \quad (13)$$

The simplest model for the dissolution of the alloy in the limiting-current region is that in which it is assumed that $CuCl_2^-$ is saturated within the CuCl porous film. This means that the flux of $CuCl_2^-$ within the film is zero, so that all the $CuCl_2^-$ that is detected at the ring, is formed by the reaction with the film at the film–solution interface. The kinetics of the dissolution of the alloy are similar to those for the dissolution of copper, *ie* proportional to $[Cl^-]$ and $\omega^{0.38}$. Therefore, the derivation of the kinetics of dissolution of the alloy follows that for the dissolution of copper. The concentration gradient of $CuCl_2^-$ in the diffusion boundary layer is described by the convective diffusion equation,

$$\frac{\partial C_1'}{\partial t} = D_1' \frac{\partial^2 C_1'}{\partial x'^2} - v_{x'} \frac{\partial C_1'}{\partial x'}, \quad x' > 0. \quad (14)$$

The origin of the x-coordinate is taken at the Cu–CuCl interface, while that of x' is taken at the CuCl–solution interface (*ie* $x' = x - \delta_f$). C_1' is the concentration of $CuCl_2^-$ in the solution. D_1' is the diffusion coefficient of $CuCl_2^-$.

The concentration gradient of Cl^- in the porous layer is determined by molecular diffusion,

$$\frac{\partial C_2}{\partial t} = D_2 \frac{\partial^2 C_2}{\partial x^2}, \quad 0 > x > \delta_f, \quad (15)$$

where C_2 is the concentration of Cl^-, and D_2 is the diffusion coefficient of Cl^- in the porous layer.

These differential equations are subject to the following boundary conditions:

$$x' = 0, N_1'(0) = k_4 C_2(\delta_f) - k_{-4} C_1'(0) \quad (16)$$

$$x' = \infty, C_1'(\infty) = 0 \quad (17)$$

$$x = 0, N_2(0) = \frac{i}{F} \quad (18)$$

$$x = \delta_f, C_2(\delta_f) = C_b. \quad (19)$$

The rate of formation of $CuCl_{ads}$ is governed by the mass balance equation

$$\frac{d\theta}{dt} = \frac{i}{F} - k_3\theta, \quad (20)$$

while the formation and dissolution of the porous film is given by the mass balance equation,

$$\rho_{CuCl}(1-\epsilon)\frac{d\delta_f}{dt} = k_3\theta - k_4 C_b + k_{-4} C_1'(0), \quad (21)$$

where ϵ is the voidage of the porous film, ρ_{CuCl} is the molar density of CuCl.

It is assumed that the crystalline CuCl that precipitates on the surface of the electrode is not electrically conductive; therefore, the electrochemical reaction can only take place on the bare alloy surface. In addition, it is assumed that at these potentials, reaction (2) will proceed in the forward direction only, so that equation (7) becomes

$$\frac{i}{F} = k_1(1-\theta)C_2(0). \quad (22)$$

Integrating equation (15) with boundary conditions (18) and (19), and combining the solution with equations (20) and (22) gives

$$\frac{i}{F} = \frac{C_b}{1/k_1 + \delta_f/D_2}. \quad (23)$$

Since we have assumed that no $CuCl_2^-$ is formed at the Cu surface, $k_4 C_b - k_{-4} C_1'(0)$ is the flux of $CuCl_2^-$ from the disk, and this flux is detected as the ring current when the ring potential is set to 610 mV. If we solve equation (14) and substitute the boundary conditions, equations (16) and (17), we get an expression for the flux of $CuCl_2^-$ from the disk. Combining this expression for the flux of $CuCl_2^-$ from the disk with equation (21) gives an expression for δ_f,

$$\frac{\delta_f}{D_2} = \frac{\delta}{D_1'}\frac{k_{-4}}{k_4} - \frac{1}{k_1}. \quad (24)$$

Substituting equation (24) into equation (23) gives an expression for the limiting-current density in terms of the observed variables,

$$\frac{i}{F} = \frac{C_b k_4 \omega^{1/2}}{\tau k_{-4}}. \quad (25)$$

Figures 12 and 13 show that equation (25) describes the dissolution kinetics in the limiting-current region.

CONCLUSIONS

The anodic dissolution of 90% Cu–10% Ni alloy in HCl solutions has been studied, and mechanisms for the dissolution have been developed. This work has shown that the dissolution of the alloy at steady state follows kinetics similar to those for pure copper. The dissolution of both copper and nickel from the alloy in the apparent-Tafel region have similar kinetic parameters to those of pure copper in the apparent-Tafel region, while the dissolution of these components from the alloy in the limiting-current region have kinetic parameters similar to the dissolution of pure components.

Acknowledgement—This project was initiated at MINTEK, Randburg, and some of the experimental work was completed at MINTEK.

REFERENCES

1. H. Uhlig, *Electrochim. Acta* **16,** 1939 (1971).
2. J. O'M. Bockris, B. T. Rubin, A. Despic and B. Lovrecek, *Electrochim. Acta* **17,** 973 (1972).
3. M. E. Walton and P. A. Brook, *Corros. Sci.* **17,** 317 (1977).
4. M. E. Walton and P. A. Brook, *Corros. Sci.* **17,** 593 (1977).
5. R. F. North and M. J. Pryor, *Corros. Sci.* **10,** 297 (1970).
6. L. Elford, F. Muller and O. Kubaschewski, *Ber. Bunsenges. Phys. Chem.* **73,** 601 (1969).
7. T. Sakurai, T. Hashizume, A. Kobayashi, A. Sakai, S. Hyodo, Y. Kuk and H. W. Pickering, *Phys. Rev. B,* **34,** 8379 (1986).
8. M. Matsuyama and T. J. Takeuchi, *Phys. Chem.* **89,** 3873 (1985).
9. H. P. Lee and K. Nobe, *J. electrochem. Soc.* **133,** 2035 (1986).
10. M. Braun and K. Nobe, *J. electrochem. Soc.* **126,** 1666 (1979).
11. W. H. Smyrl, *J. electrochem. Soc.* **132,** 1555 (1985).
12. R. S. Cooper and J. H. Bartlett, *J. electrochem. Soc.* **105,** 109 (1958).
13. C. H. Bonfiglio, H. C. Albaya and O. A. Cobo, *Corros. Sci.* **13,** 717 (1973).
14. A. Moreau, *Electrochim. Acta* **26,** 497 (1981).
15. A. Moreau, J. P. Frayret, F. Delrey and R. Pointeau, *Electrochim. Acta* **27,** 1281 (1982).
16. H. P. Lee, K. Nobe and A. Pearlstein, *J. electrochem. Soc.* **132,** 1031 (1985).
17. A. Pearlstein, H. P. Lee, and K. Nobe, *J. electrochem. Soc.* **132,** 2159 (1985).
18. A. Bengali and K. Nobe, *J. electrochem. Soc.* **126,** 1118 (1979).